

# Growth index in an accelerating universe.

Seokcheon Lee<sup>1,2</sup> and Kin-Wang Ng<sup>1,2,3</sup>

June 27, 2019

<sup>1</sup>*Institute of Physics, Academia Sinica, Taipei, Taiwan 11529, R.O.C.*

<sup>2</sup>*Leung Center for Cosmology and Particle Astrophysics, National Taiwan University, Taipei, Taiwan 10617, R.O.C.*

<sup>3</sup>*Institute of Astronomy and Astrophysics, Academia Sinica, Taipei, Taiwan 11529, R.O.C.*

## Abstract

We find the exact analytic solution of the linear density perturbation  $\delta$  for any given value of constant equation of state of dark energy  $\omega_{de}$ . We also obtain the exact analytic form of growth index ( $f = \Omega_m(a)^\gamma$ ) at present epoch in a flat universe with including  $\omega_{de}$  from this solution of  $\delta$ . For the cosmological constant ( $\omega_{de} = -1$ ) we obtain  $\gamma = 0.5547$  which is very close to the well known value  $6/11$ . However, if  $\omega_{de} = -0.9$ , then  $\gamma$  gives rise to 0.6405.  $\Omega_m^0$  dependence of  $\gamma$  is fairly small for the viable range of the current matter energy density  $0.2 \leq \Omega_m^0 \leq 0.3$ . (0.6% and 3% changes in  $\gamma$  for  $\omega_{de}$  equal to  $-1$  and  $-0.9$ , respectively.) The difference of peculiar velocity values from the different choices of  $\gamma$  is about 11% for  $\Omega_m^0 = 0.3$ . This simple but accurate formula which covers a large class of dark energy models will provide a practical tool for galaxy redshift survey to measure the matter density and the peculiar velocity.

The background evolution equations in a flat Friedmann-Robertson-Walker universe ( $\rho_m + \rho_{de} = \rho_{cr}$ ) are

$$\left(\frac{\dot{a}}{a}\right)^2 = \frac{8\pi G}{3}(\rho_m + \rho_{de}) = \frac{8\pi G}{3}\rho_{cr}, \quad (1)$$

$$2\frac{\ddot{a}}{a} + \left(\frac{\dot{a}}{a}\right)^2 = -8\pi G\omega_{de}\rho_{de}, \quad (2)$$

where  $\omega_{de}$  is the equation of state (eos) of dark energy,  $\rho_m$  and  $\rho_{de}$  are the energy densities of the matter and the dark energy, respectively. We

consider the constant  $\omega_{de}$  only. The dark energy does not participate directly in cluster formation, but it alters the cosmic evolution of the background. The linear density perturbation of the matter ( $\delta = \delta\rho_m/\rho_m$ ) for sub-horizon scales is governed by [1]

$$\ddot{\delta} + 2\frac{\dot{a}}{a}\dot{\delta} = 4\pi G\rho_m\delta. \quad (3)$$

It is well known that the growing mode (Heath) solution of the above equation (3) is [2]

$$\delta_{\text{hsk}} = CH_0^{-2}a^{-1}X^{1/2}\int_0^a X^{-3/2}(a')da', \quad (4)$$

where  $X = (aH/H_0)^2 = \Omega_m^0 a^{-1} + \Omega_{de}^0 a^{-1-3\omega_{de}}$ ,  $\Omega_m^0 = \rho_m^0/\rho_{cr}^0$  and  $\Omega_{de}^0 = 1 - \Omega_m^0$  are the present energy density contrast of the matter and the dark energy, respectively. Actually, this solution is known as exact only for  $\omega_{de} = -1/3$  and/or  $-1$  (see Appendix A and the reference) [3]. However, when we replace this solution into the evolution equation (3) we have the second order inhomogeneous differential equation

$$\ddot{\delta}_{\text{hsk}} + 2H\dot{\delta}_{\text{hsk}} - 4\pi G\rho_m\delta_{\text{hsk}} - \left[4\pi G(1 + \omega_{de})(1 + 3\omega_{de})\rho_{de}\right]\delta_{\text{hsk}} = 0. \quad (5)$$

We emphasize that both Eq. (3) and Eq. (5) are equal. Thus, this solution gives the homogeneous solution of equation (5) when  $\omega_{de} = -1/3$  and/or  $-1$ . In addition to this homogeneous solution, we need to find the inhomogeneous solution. We find the exact analytic inhomogeneous solution (we call it ‘‘sky-kin’’ solution  $\delta_{sk}$ ) of this equation (see also Appendix A for details). Thus, for any given value of constant  $\omega_{de}$  we have

$$\begin{aligned} \delta_{\text{hsk}} &= \delta_{\text{h}} + \delta_{\text{sk}} \quad \text{where } Y = -\frac{\omega_{de}}{2(1 + \omega_{de})}\Omega_{de}^0 a^{-3(1 + \omega_{de})} \text{ and} \\ \delta_{\text{sk}}(a, \omega_{de}, \Omega_{de}^0) &= a\left(-\frac{3}{2}\omega_{de}\Omega_{de}^0\right)^{\frac{-1}{3(1 + \omega_{de})}} A_L\left(L\left[1 + \frac{2}{3(1 + \omega_{de})}, -\frac{5}{6(1 + \omega_{de})}, Y\right]\right. \\ &\quad \left. - \frac{L[2, -5/4, Y]}{F_c[-2, -1/4, Y]} F_c\left[-1 - \frac{2}{3(1 + \omega_{de})}, 1 - \frac{5}{6(1 + \omega_{de})}, Y\right]\right). \end{aligned} \quad (6)$$

$\delta_{\text{h}}$  is the well known homogeneous solution for  $\omega_{de} = -1$  and/or  $-1/3$ ,  $L$  and  $F_c$  are the Laguerre polynomials and the confluent hypergeometric series, respectively.  $Y$  is positive for  $\omega_{de} > -1$ , thus both function are well defined in this range of  $\omega_{de}$ . In appendix A, we show that  $\delta_{sk}$  gives the decaying

mode for the suitable choice of  $\omega_{de}$  instead of growing one and thus we can ignore this correction term. This check is important to make sure that equation (4) is the real growing mode solution for the given value of  $\omega_{de}$  [4]. The growth index  $f$  is defined as

$$f = \frac{d \ln \delta}{d \ln a} \equiv \Omega_m(a)^\gamma, \quad (7)$$

Thus,  $f$  is expressed from the equation (4) by

$$f(\Omega_m^0, \Omega_{de}^0, \omega_{de}, a) = -\frac{3}{2} - \frac{3\omega_{de}\Omega_{de}^0 a^{-1-3\omega_{de}}}{2X} + \frac{aX^{-3/2}(a)}{\int_0^a X^{-3/2}(a')da'}. \quad (8)$$

We can find the exact analytic solutions of the above equation at the present epoch ( $a = 1$ ,  $X(a = 1) = 1$ )

$$f(\Omega_m^0, \Omega_{de}^0, \omega_{de}, 1) = -\frac{3}{2} - \frac{3}{2}\omega_{de}\Omega_{de}^0 - 3\omega_{de}(\Omega_m^0)^{3/2} \frac{\Gamma[1 - \frac{5}{6\omega_{de}}]}{\Gamma[\frac{-5}{6\omega_{de}}]\Gamma[1]} \frac{1}{F[\frac{3}{2}, \frac{-5}{6\omega_{de}}, 1 - \frac{5}{6\omega_{de}}, -\frac{\Omega_{de}^0}{\Omega_m^0}]}, \quad (9)$$

where  $\Gamma$  is the gamma function and  $F$  is the hypergeometric function. For  $\Omega_m^0 = 1$  one get  $f = 1$  for all  $a$ , which is consistent with  $\delta \propto a$ . Also we compare the result with a non-flat without the cosmological constant  $f = -1 - \Omega_m^0/2 + 5/2(\Omega_m^0)^{3/2}/F[3/2, 5/2, 7/2, 1 - (\Omega_m^0)^{-1}]$  as shown in the reference [5]. In Fig. 1, we show the present value of growth index  $f(\Omega_m^0, a = 1)$  as a function of  $\Omega_m^0$ .

Dot line shows the behavior of  $f$  as a function of  $\Omega_m^0$  when we adopt  $\gamma = 6/11$  [6]. We can find the present value of parameter  $\gamma = \ln f(a = 1)/\ln \Omega_m^0$ . The dash-dot line represents  $f$  with  $\gamma = 0.5547$ , which we get from the above relation when we choose  $\omega_{de} = -1$  and  $\Omega_m^0 = 0.3$ . This new  $\gamma$  value gains 1 – 2 % accuracy compared to  $\gamma = 6/11$  for  $0.2 \leq \Omega_m^0 \leq 0.3$ . The solid line shows the exact analytic solution of  $f$  when we choose  $\omega_{de} = -1$ . The other exact solution of  $f$  with  $\omega_{de} = -0.9$  is depicted as a dash line. When we fit this value in the relation we can find  $\gamma = 0.6405$  and this curve is described by dash-dot-dot line in the Fig. 1. This  $\gamma$  value gives a good approximation on proper values of  $\Omega_m^0$ . However, the behavior of  $f$  with this  $\gamma$  value shows the discrepancy with the exact solution at low  $\Omega_m^0$ . We will explain this in the below.

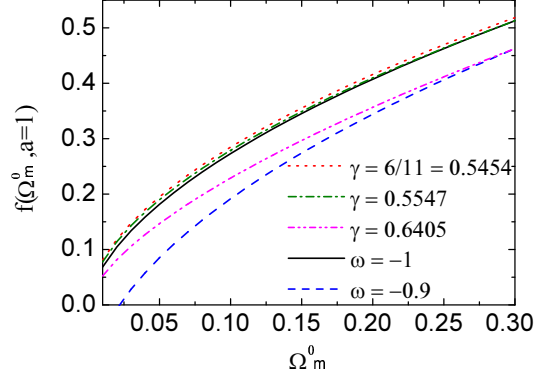


Figure 1: The behaviors of  $f$  for the different models. Dot line, dash-dot line, and dash-dot-dot line correspond to when we choose  $\gamma$  in the equation (7) as  $6/11$ ,  $0.5547$ , and  $0.6405$ , respectively. Solid line and dash line represent the behaviors of exact analytic solutions of  $f$  in the equation (9) when we choose  $\omega_{de}$  as  $-1$  and  $-0.9$ , respectively.

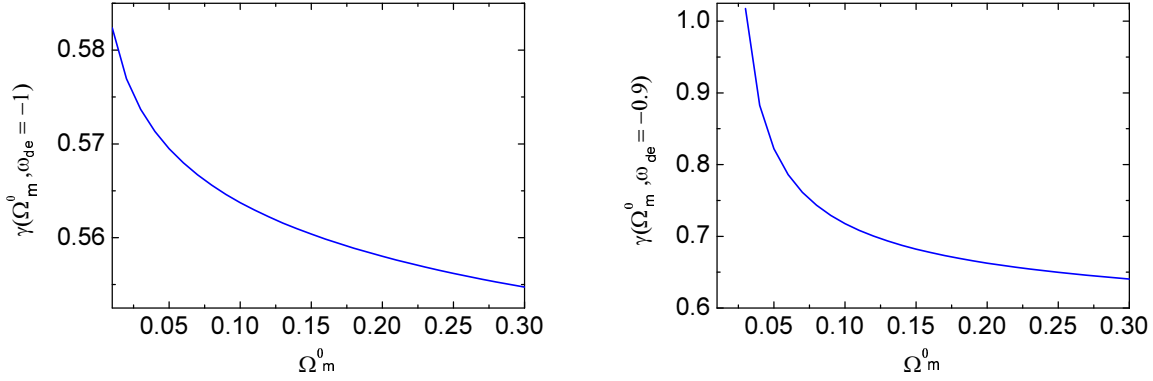


Figure 2:  $\gamma = \ln f / \ln \Omega_m^0$ . a) The values of  $\gamma$  as a function of  $\Omega_m^0$  when  $\omega_{de} = -1$ . b) The dependence of  $\gamma$  on  $\Omega_m^0$  when  $\omega_{de} = -0.9$ .

We show the  $\Omega_m^0$  dependence of this parameter ( $\gamma$ ) for the different values of  $\omega_{de}$  in the figure 2. For  $\omega_{de} = -1$ ,  $\gamma$  is insensitive to the change in  $\Omega_m^0$  as shown in Fig. 2a. However, we see that  $\gamma$  dependence on  $\Omega_m^0$  is not negligible for small  $\Omega_m^0$  when  $\omega_{de} = -0.9$  from Fig. 2b. We can understand this property from the equations (7) and (9)

$$\gamma(\Omega_m^0, \omega_{de}) = \frac{\ln\left[-\frac{3}{2}(1 + \omega_{de}) - \frac{3}{2}\omega_{de}\Omega_m^0 - 3\omega_{de}(\Omega_m^0)^{3/2} \frac{\Gamma[1-\frac{5}{6\omega_{de}}]}{\Gamma[\frac{-5}{6\omega_{de}}]\Gamma[1]} / F\left[\frac{3}{2}, \frac{-5}{6\omega_{de}}, 1 - \frac{5}{6\omega_{de}}, -\frac{\Omega_{de}^0}{\Omega_m^0}\right]\right]}{\ln \Omega_m^0} . \quad (10)$$

When  $\omega_{de} = -1$ , the first term of the numerator in the above equation becomes 0. And the third term in the numerator dominates the second one. Thus, the dependence on  $\Omega_m^0$  is proportional to  $\ln((\Omega_m^0)^{3/2}/F[1 - (\Omega_m^0)^{-1}])/\ln(\Omega_m^0)$ . However, if  $\omega \neq -1$ , then the first term of the numerator does not disappear and gives the correction being proportional to  $1/\ln(\Omega_m^0)$  in addition to  $\ln((\Omega_m^0)^{3/2}/F[1 - \Omega_m^0])/\ln(\Omega_m^0)$ . And the first term is much sensitive to the variation of  $\Omega_m^0$  than the third one. Thus, we have almost  $\Omega_m^0$  independent  $\gamma$  for  $\omega_{de} = -1$ . However,  $\gamma$  can be sensitive to  $\Omega_m^0$  when  $\omega_{de} \neq -1$ . However,  $\gamma$  is almost independent from  $\Omega_m^0$  for the proper values of present matter density contrast  $0.2 \leq \Omega_m^0 \leq 0.3$ . In both cases, we get the higher  $\gamma$  values for the smaller values of  $\Omega_m^0$ .

We also show the  $\gamma$  dependence on  $\omega_{de}$  for the different values of  $\Omega_m^0 = 0.24, 0.30$  in Fig. 3. For the bigger value of  $\omega_{de}$  we obtain the bigger value of  $\gamma$ . These higher values are still consistent with a recent analysis  $\gamma = 0.6_{-0.3}^{+0.4}$  through [7]. Also as a consistent check, we can find the higher values of  $\gamma$  for the smaller value of  $\Omega_m^0$  as same as in Fig. 2. We can numerically evaluate the value of  $\gamma$  at any redshift,  $z = a^{-1} - 1$  from the equation (8). We obtain  $f(\Omega_m^0 = 0.3, \omega_{de} = -1, z = 0.15) = 0.5982$  and  $f(\Omega_m^0 = 0.3, \omega_{de} = -0.9, z = 0.15) = 0.5481$ . Both are consistent with the 2dF Galaxy Redshift Survey (2dFGRS)  $f(\Omega_m^0 = 0.3, \omega_{de} = -1, z = 0.15) = 0.51 \pm 0.15$  [8].

In linear theory, the peculiar velocity  $\vec{v}_{pec}$  is related to the peculiar acceleration  $\vec{g}$  and/or interior average overdensity  $\langle \delta \rangle_R$  in a spherical perturbation of radius  $R$  [9]

$$|\vec{v}_{pec}| = \frac{2}{3} \left| \frac{f\vec{g}}{H\Omega_m^0} \right| = \frac{1}{3} H R f \langle \delta \rangle_R . \quad (11)$$

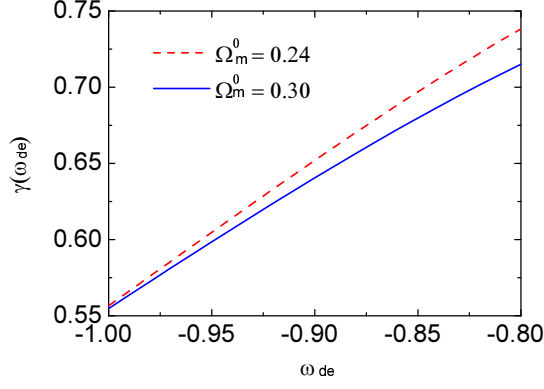


Figure 3: The  $\gamma$  dependence on  $\omega_{de}$  with different values of  $\Omega_m^0 = 0.24, 0.30$ .

The difference of this peculiar velocity between two different values of  $\gamma$ s for  $\omega_{de} = -1, -0.9$  is about 11% when we choose  $\Omega_m^0 = 0.3$ . Thus, the accurate parameter value  $\gamma$  especially for  $\omega_{de} \neq -1$  will provide the better analysis tool for galaxy redshift survey.

## A Appendix

We replace the growing mode solution (4) into the equation (3) to get

$$\begin{aligned} \ddot{\delta} + 2H\dot{\delta} - 4\pi G\rho_m\delta &= 0 \\ = \ddot{\delta}_{\text{hsk}} + 2H\dot{\delta}_{\text{hsk}} - 4\pi G\rho_m\delta_{\text{hsk}} - \left[4\pi G(1 + \omega_{de})(1 + 3\omega_{de})\rho_{de}\right]\delta_{\text{hsk}} \end{aligned} \quad (12)$$

Thus, the equation (4) gives the homogeneous solution when  $\omega_{de} = -1$  and/or  $-1/3$ . The above inhomogeneous second order differential equation (12) has both homogeneous and inhomogeneous solutions ( $\delta_{\text{hsk}} = \delta_{\text{h}} + \delta_{\text{sk}}$ ). We solve the inhomogeneous solution ( $\delta_{\text{sk}}$ ) by using new parameters  $T = (3/2)(1 + s/3)\Omega_{de}^0 a^s$  and  $s = -3(1 + \omega_{de})$ . After replacing these parameters in the inhomogeneous equation (12), we have

$$T \frac{d^2 \delta_{\text{I}}}{dT^2} + \left[1 + \frac{1}{2s} + \frac{T}{s}\right] \frac{d\delta_{\text{I}}}{dT} + \left[\frac{1-s}{s^2} - \frac{3}{2s^2 T}\right] \delta_{\text{I}} = 0. \quad (13)$$

Now we put  $\delta_1(T) = T^{1/s}D(T) = (-sY)^{1/s}B(Y) = \delta_1(Y)$  where  $Y = -T/s$ , then the above equation (13) becomes

$$Y \frac{d^2 B}{dY^2} + \left( \frac{5}{2s} + 1 - Y \right) \frac{dB}{dY} + \frac{s-2}{s} B = 0. \quad (14)$$

This equation (14) is nothing but the confluent hypergeometric (*i.e.* Kummer's) equation. Thus, the inhomogeneous solution  $\delta_1$  ( we define as  $\delta_{sk}$ ) of equation (12) is

$$\delta_{sk}(s, Y) = (-sY)^{\frac{1}{s}} \left( A_L L \left[ \frac{-2+s}{s}, \frac{5}{2s}, Y \right] + A_F F_c \left[ \frac{2-s}{s}, 1 + \frac{5}{2s}, Y \right] \right), \quad (15)$$

where  $A_{L,F}$  are arbitrary constants,  $L$  is the Laguerre polynomials, and  $F_c$  is the confluent hypergeometric series [10]. Laguerre polynomials are well defined in range  $0 \leq Y < \infty$ . Also we can find the relation between  $A_L$  and  $A_F$  from the fact that  $\delta_{sk} = 0$  for  $\omega_{de} = -1/3$  (*i.e.* only homogeneous solution exists for this  $\omega_{de}$ ). This gives us

$$A_F = -\frac{L \left[ 2, -\frac{5}{4}, Y \right]}{F_c \left[ -2, -\frac{1}{4}, Y \right]} A_L = -0.5 A_L, \quad (16)$$

for  $0 \leq a \leq 1$ . In Fig. 4, we show the behaviors of this sky-kin solution (*i.e.*  $\delta_{sk}$  in Eq. (6)) for  $\omega_{de} = -0.9$  and  $-0.8$  when we choose  $\Omega_{de}^0 = 0.7$ . We use  $A_L = -1$  in this figure. The solid line shows the evolution of  $\delta_{sk}$  when we choose  $\omega_{de} = -0.9$ . With  $\omega_{de} = -0.8$ ,  $\delta_{sk}$  evolution is depicted as the dash line. Both show the decaying modes. Thus, we can use (4) as an exact growing mode solution in these values of  $\omega_{de}$ .

From the equation (8), we need to solve the integration to find the analytic form of  $f$  at present epoch [11],

$$\begin{aligned} \int_0^1 \frac{da}{X^{3/2}(a)} &= \int_0^1 \frac{da}{(\Omega_m^0 a^{-1} + \Omega_{de}^0 a^{-1-3\omega_{de}})^{3/2}} = \int_0^1 \frac{da}{(1 + \Omega_{de}^0 / \Omega_m^0 a^{-3\omega_{de}})^{3/2} (\Omega_m^0 / a)^{3/2}} \\ &= \frac{-1}{3\omega_{de} (\Omega_m^0)^{3/2}} \int_0^1 \eta^{-1-5/(6\omega_{de})} (1 - r\eta)^{-3/2} d\eta \\ &= \frac{-1}{3\omega_{de} (\Omega_m^0)^{3/2}} \frac{\Gamma[\frac{-5}{6\omega_{de}}] \Gamma[1]}{\Gamma[1 - \frac{5}{6\omega_{de}}]} F \left[ \frac{3}{2}, \frac{-5}{6\omega_{de}}, 1 - \frac{5}{6\omega_{de}}, -\frac{\Omega_{de}^0}{\Omega_m^0} \right], \end{aligned} \quad (17)$$

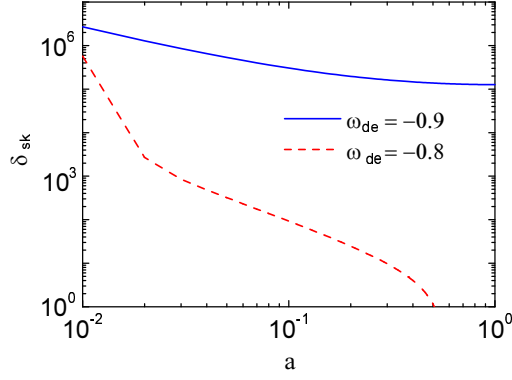


Figure 4: The evolution of the inhomogeneous solution  $\delta_I$  for  $\omega_{de} = -0.9$  and  $-0.8$ .

where we use  $a^{-3\omega_{de}} = \eta$  and  $r = -\Omega_{de}^0/\Omega_m^0 = 1 - (\Omega_m^0)^{-1}$ . We can also check the result of a non-flat universe without the cosmological constant in the reference [5]. In this case we have  $k/H_0^2 \equiv \Omega_K = (1 - \Omega_m^0)$ . Then we obtain the expression for  $X = \Omega_m^0 a^{-1} + \Omega_K$ . Mathematically, this is the same as the dark energy case with the equation of state of the dark energy  $\omega_{de} = -1/3$ . Then the above integral (17) becomes

$$\int_0^1 \frac{da}{X^{3/2}(a)} = \frac{1}{(\Omega_m^0)^{3/2}} \frac{\Gamma[\frac{5}{2}]\Gamma[1]}{\Gamma[\frac{7}{2}]} F\left[\frac{3}{2}, \frac{5}{2}, \frac{7}{2}, -\frac{\Omega_K}{\Omega_m^0}\right] = \frac{2}{5} (\Omega_m^0)^{-3/2} F\left[\frac{3}{2}, \frac{5}{2}, \frac{7}{2}, 1 - (\Omega_m^0)^{-1}\right]. \quad (18)$$

Thus, we can reproduce  $f = -1 - \Omega_m^0/2 + 5/2(\Omega_m^0)^{3/2}/F[\frac{3}{2}, \frac{5}{2}, \frac{7}{2}, 1 - (\Omega_m^0)^{-1}]$  in a non-flat without cosmological constant case.

## References

- [1] W. B. Bonnor, Mon. Not. R. Astr. Soc. **117**, 104 (1957).
- [2] D. J. Heath, Mon. Not. Roy. Astron. Soc. **179**, 351 (1977).
- [3] V. Sahni and P. Coles, Phys. Rep. **262**, 1 (1995) [arXiv:astro-ph/9505005], U. Alam, V. Sahni, and A. A. Starobinsky, [arXiv:0812.2846].



- [4] E. V. Linder and A. Jenkins, *Mon. Not. Roy. Astron. Soc.* **346**, 573 (2003) [arXiv:astro-ph/0305286].
- [5] O. Lahav, P. B. Lilje, J. R. Primack, and M. J. Rees, *Mon. Not. R. Astr. Soc.* **251**, 128 (1991).
- [6] L. Wang and P. J. Steinhardt, *Astrophys. J.* **508**, 483 (1998) [arXiv:astro-ph/9804015].
- [7] C. Di Porto and L. Amendola, *Phys. Rev. D* **77**, 083508 (2008) [arXiv:0707.2686].
- [8] E. Hawkins *et. al.*, *Mon. Not. R. Astr. Soc.* **346**, 78 (2003) [arXiv:astro-ph/0212375], L. Verde *et. al.*, *Mon. Not. R. Astr. Soc.* **335**, 432 (2002) [arXiv:astro-ph/0112161].
- [9] P. J. E. Peebles, *Large Scale Structure of the Universe*, Princeton University Press, Princeton (1980).
- [10] P. M. Morse and H. Feshbach, *Methods of Theoretical Physics, Part I*, McGraw-Hill Science, New York (1953).
- [11] M. Abramowitz and I. A. Stegun, *Handbook of Mathematical Functions with Formulas, Graphs, and Mathematical Tables*, Dover Publications, New York (1970).